Antitumor activity and pharmacokinetic properties of PF-00299804, a second-generation irreversible pan-erbB receptor tyrosine kinase inhibitor

Andrea J. Gonzales,[1] Kenneth E. Hook,[1] Irene W. Althaus,[1] Paul A. Ellis,[1] Erin Trachet,[1] Amy M. Delaney,[1] Patricia J. Harvey,[1] Teresa A. Ellis,[1] Danielle M. Amato,[1] James M. Nelson,[1] David W. Fry,[1] Tong Zhu,[2] Cho-Ming Loi,[2] Stephen A. Fakhoury,[3] Kevin M. Schlosser,[3] Karen E. Sexton,[3] R. Thomas Winters,[3] Jessica E. Reed,[3] Alex J. Bridges,[3] Daniel J. Lettiere,[4] Deborah A. Baker,[4] Jianxin Yang,[4] Helen T. Lee,[3] Haile Tecle,[3] and Patrick W. Vincent[4]

[1]Cancer Biology, [2]Pharmacokinetics & Drug Metabolism, and [3]Chemistry, Pfizer Global Research and Development, Ann Arbor, Michigan; and [4]Cancer Biology, Pfizer Global Research and Development, Groton, Connecticut

Abstract

Signaling through the erbB receptor family of tyrosine kinases contributes to the proliferation, differentiation, migration, and survival of a variety of cell types. Abnormalities in members of this receptor family have been shown to play a role in oncogenesis, thus making them attractive targets for anticancer treatments. PF-00299804 is a second-generation irreversible pan-erbB receptor tyrosine kinase inhibitor currently in phase I clinical trials. PF-00299804 is believed to irreversibly inhibit erbB tyrosine kinase activity through binding at the ATP site and covalent modification of nucleophilic cysteine residues in the catalytic domains of erbB family members. Oral administration of PF-00299804 causes significant antitumor activity, including marked tumor regressions in a variety of human tumor xenograft models that express and/or overexpress erbB family members or contain the double mutation (L858R/T790M) in erbB1 (EGFR) associated with resistance to gefitinib and erlotinib. Furthermore, PF-00299804 shows exceptional distribution to human tumor xenografts and excellent pharmacokinetic properties across species. [Mol Cancer Ther 2008;7(7):1880–9]

Received 10/29/07; revised 3/5/08; accepted 4/3/08.

The costs of publication of this article were defrayed in part by the payment of page charges. This article must therefore be hereby marked *advertisement* in accordance with 18 U.S.C. Section 1734 solely to indicate this fact.

Requests for reprints: Andrea J. Gonzales, Discovery Biology and Internal Medicine, Pfizer, Inc., 7000 Portage Road, KZO-300-4-406.4, Kalamazoo, MI 49001. Phone: 269-833-4146; Fax: 269-833-7721.
E-mail: Andrea.Gonzales@pfizer.com

doi:10.1158/1535-7163.MCT-07-2232

Introduction

The erbB receptor tyrosine kinase family, whose members include erbB1 (EGFR, HER1), erbB2 (neu, HER2), erbB3 (HER3), and erbB4 (HER4), consists of transmembrane glycoproteins that transduce extracellular signals to the nucleus when activated upon ligand binding. Activation of these receptor tyrosine kinases leads to important phenotypic changes such as proliferation, survival, adhesion, migration, and invasion, all of which play an important role in the cancer process. Abnormalities in erbB family members, such as overexpression of receptors and/or ligands, amplification, truncations, and activating mutations have been well-documented in a variety of human tumor types. Many groups have shown that patients with tumors harboring abnormalities in these receptors (e.g., amplification of erbB2 in breast cancers) or patients with tumors that coexpress more than one erbB family member have a worse outcome than those with no abnormalities in this receptor family. These findings make the erbB family of receptor tyrosine kinases attractive targets for potential anticancer therapies (1–4).

Numerous erbB receptor tyrosine kinase inhibitors are currently in clinical development. Three such inhibitors have been approved for use in cancer patients: gefitinib (ZD-1839, Iressa; ref. 5), erlotinib (OSI-774, Tarceva; ref. 6), and lapatinib (GW572016, Tykerb; ref. 7). All three are quinazoline-based reversible inhibitors. Gefitinib and erlotinib are reported to be highly selective toward epidermal growth factor receptor (EGFR) with little activity toward other EGFR family members (8, 9), whereas lapatinib is a dual erbB1/erbB2 inhibitor (10). All three inhibit the tyrosine kinase activity of EGFR and/or erbB2 in a number of human tumor cell lines and show antitumor activity as a single agent (8–10) or in combination with cytotoxic agents (11–13) in a variety of human tumor xenograft models. Currently, gefitinib and erlotinib have been approved in multiple countries for use in patients with chemotherapy-refractory non–small cell lung cancer (NSCLC), whereas lapatinib has been approved for use in combination with capecitabine in patients with advanced or metastatic HER2-positive breast cancer who have received prior therapy. Therefore, targeting this receptor family is a proven anticancer strategy (7, 14).

An intriguing retrospective finding from patients with NSCLC treated with gefitinib or erlotinib shows that the population of patients responding to these reversible EGFR inhibitors contained somatic mutations in the kinase domain of EGFR. These mutations have been shown to increase sensitivity to gefitinib and erlotinib *in vitro*, and may predict sensitivity to reversible inhibitors in the clinical setting (15–19). Patients who initially responded

to gefitinib or erlotinib, but then subsequently relapsed, were found to have gained a secondary mutation (T790M) in the kinase domain of EGFR. This mutation has been shown to confer resistance to inhibition by gefitinib or erlotinib in cell culture systems likely due to conformational changes that lead to the steric hindrance of gefitinib or erlotinib binding (20, 21). Additional mutations in EGFRs, which have been reported by various groups, have led to resistance to reversible anilinoquinazolines (20, 21). Interestingly, these mutated receptors seem to be sensitive to irreversible EGFR inhibitors, suggesting that irreversible inhibitors may have utility in patients with tumors that have acquired resistance to gefitinib or erlotinib (21, 22).

This report discloses the pharmacology of PF-00299804, a second-generation irreversible pan-erbB receptor tyrosine kinase inhibitor, and provides evidence that this compound can potently inhibit wild-type erbB receptors as well as a mutated form of EGFR associated with *in vivo* resistance to gefitinib or erlotinib. We describe excellent oral antitumor activity with this agent in a variety of human tumor xenograft models. We also show that this compound can produce complete regressions in some tumor types, likely due to the prolonged pharmacodynamic effects within the tumor that correlate with marked distribution of compound to the target tissue. Finally, PF-00299804 shows superior antitumor activity and pharmacokinetic properties when compared with its predecessor, CI-1033.

Materials and Methods

Chemicals

PF-00299804, CI-1033, erlotinib (CP-358,744; Tarceva, OSI Pharmaceuticals), and gefitinib (ZD 1839; Iressa, AstraZeneca) were synthesized in the laboratories of Pfizer Global Research and Development (Ann Arbor, MI and Groton CT).

Cell Culture

All cells, unless noted, were cultured in DMEM/F12 medium (Life Technologies) containing 10% fetal bovine serum (Life Technologies) and 10 ng/mL of gentamicin (Life Technologies). Cells were incubated at 37°C in 5% CO_2.

Irreversibility Assessments for PF-00299804

To assess the irreversibility of enzyme inhibition by PF-00299804, 167 nmol/L of GST-erbB1 (23) was preincubated with 825 nmol/L of PF-00299804 for 30 min on ice then diluted 167-fold (final concentration in the reaction was 1 nmol/L GST-erbB1 and 5 nmol/L PF-00299804). Enzyme activity was assessed using the ELISA-based enzyme assay format previously described (23). Staurosporine, a reversible ATP-competitive inhibitor of kinases, was used at identical concentrations as PF-00299804 and served as a control in the studies. Results were plotted as a percentage of the activity relative to DMSO controls using GraphPad Prism 4.00 software (GraphPad Software, Inc.).[5]

To determine whether PF-00299804 could irreversibly inhibit EGF-induced phosphorylation of EGFR in cells, a sandwich ELISA approach with BioVeris technology using A431 squamous carcinoma cells was employed as described previously (23). In general, A431 cells were incubated with 2 μmol/L of PF-00299804 for varying lengths of time (1, 5, 30, 60, or 120 min). Medium was removed, and cells were repeatedly washed thrice with serum-free and inhibitor-free medium every hour for 2 h. After the last wash, cells were stimulated with 100 ng/mL of EGF (Sigma) for 5 min at 37°C, and phosphorylation of EGFR was assessed.

Inhibition of Receptor Autophosphorylation in A431 Cells

Immunoblotting procedures were used to assess the *in vitro* inhibition of EGF-induced receptor autophosphorylation in the A431 squamous cell carcinoma line by PF-00299804. Procedures followed those previously described (24). To detect phosphorylated erbB1, anti–phosphorylated erbB1 (Tyr^{1068}) from Cell Signaling Technology was diluted in blocking buffer [3% bovine serum albumin, 50 mmol/L Tris (pH 8.0), 150 mmol/L NaCl, 0.1% Tween 20, 10 mmol/L β-glycerophosphate, 1 mmol/L NaF, and 0.1 mmol/L Na_3VO_4] according to the instructions of the manufacturer. Total erbB1 was detected using an anti-erbB1 (sc-03) antibody from Santa Cruz Biotechnology diluted in Blotto (Pierce Biotechnology) according to the instructions of the manufacturer. Goat anti-rabbit IgG coupled with horseradish peroxidase (Bio-Rad Technologies) diluted 1:10,000 in 3% bovine serum albumin buffer or Blotto was used to detect anti–phosphorylated erbB1 or anti-erbB1, and enhanced chemiluminescence (Amersham Biosciences) was done according to the instructions of the manufacturer. Phosphorylated erbB1 signals were quantitated by densitometry using ImageQuant 5.0 software on a Molecular Dynamics Personal Densitometer SI and normalized to total erbB1. Total erbB1 was detected after stripping the phosphorylated erbB1 blot with Re-Blot Plus (Chemicon International, Inc.). Data were graphically displayed as a percentage of the activity relative to DMSO controls using GraphPad Prism 4.00, and IC_{50} curves were fitted using a nonlinear regression model with a sigmoidal dose-response.

Cell Proliferation Assays

The H1975 human NSCLC line was obtained from American Type Culture Collection and maintained according to their instructions. Cell proliferation was measured using an MTT Cell Proliferation Assay kit obtained from American Type Culture Collection and followed the manufacturer's instructions. Cell viabilities versus compound concentrations were plotted using GraphPad Prism 4.00 software. IC_{50} curves were fitted using a nonlinear regression model with a sigmoidal dose-response.

Human Tumor Xenograft Studies

Female severe combined immunodeficiency mice (Charles River Laboratories) were used for xenograft studies. The mice were housed and maintained in accordance with Pfizer Institutional Animal Care and Use

[5] http://www.graphpad.com/

Committee, State, and Federal guidelines for the humane treatment and care of laboratory animals. Mice received food and water *ad libitum*. All protocols involving animals were approved by the Pfizer Research and Development Institutional Animal Care and Use Committee. Xenograft models H125, SKOV3, and A431 were established and maintained as a serial *in vivo* passage of subcutaneous fragments (3 × 3 mm) implanted in the flank. H1975 tumors were generated by harvesting cells from mid–log phase cultures using trypsin-EDTA (Invitrogen, Inc.). Five million cells were injected s.c. into the right flank of each mouse. Treatment was initiated when tumors in mice reached a weight of 100 to 250 mg for antitumor efficacy studies and pharmacodynamic studies.

All inhibitors were given p.o. once daily for the duration indicated in the corresponding figure legend. PF-00299804 and CI-1033 were dissolved in 50 mmol/L of sodium lactate buffer (pH 4.0), and erlotinib was prepared in a 5% aqueous Gelucire (Gattefosse) stock. Tumor weight was calculated using the equation [length × $(\text{width})^2$] / 2. Treatments producing >10% lethality and/or >20% net body weight loss were considered toxic. Antitumor effects were measured as the incidence of complete regressions, partial regressions, and tumor growth delay. Complete regressions are defined as tumors that are reduced in weight to below the limit of palpation. Partial regressions are defined as tumors that are reduced by >50% but <100% of their initial weight. A minimum duration of 7 days is required for a complete regression or partial regression to be considered durable. Tumor growth delay is the median difference (in days) for the treated and control tumors to reach a specified evaluation size (25, 26).

Statistical analyses were conducted using GraphPad Prism version 4.0. The effect of compound treatment on tumor growth delays (SKOV3, A431, H125) and H1975 tumor volume changes were statistically analyzed with one-way ANOVA with individual group comparisons evaluated by Bonferroni's multiple comparison test. In both tests, $P < 0.05$ was considered significant.

In vivo Assessment of Pharmacodynamic Effects

PF-00299804, CI-1033, or erlotinib were given to mice implanted with SKOV3 or H1975 to assess modulation of the erbB target *in vivo*. For pharmacodynamic studies using the SKOV3 xenograft, mice were dosed once a day for 2 days. For studies using the H1975 xenograft, mice were dosed once a day for 14 days. Tumor samples were harvested at various times after the last dose (6, 24, and 48 h for the SKOV3 line and 6 and 26 h for the H1975 line). Excised tumors were immediately frozen in liquid nitrogen and ground into a powder over liquid nitrogen using a mortar and pestle. Powders (100–500 mg) were suspended in 0.1 to 1.5 mL of ice-cold cell lysis buffer [50 mmol/L Tris (pH 7.5), 150 mmol/L NaCl, 5 mmol/L EDTA, 50 mmol/L B-glycerophosphate, 0.1% SDS, 1% Triton, 0.2% deoxycholate, 1 mmol/L sodium vanadate, and 1 EDTA-free Complete protease inhibitor tablet from Roche] and homogenized with a Polytron hand-held tissue homogenizer. Protein concentrations were determined on clarified lysates using a Bradford Protein Assay (Bio-Rad) or BCA reagents (Pierce Biotechnology). For each sample, 50 μg of protein were denatured and separated by SDS-PAGE. Proteins were transferred to 0.2-μm nitrocellulose membranes (Invitrogen). Anti–phosphorylated erbB1 (Tyr^{1068}) from Sigma-Aldrich, Co., was used to detect phosphorylated erbB1 in the H1975 line, and anti–phosphorylated erbB2 (Tyr^{1248}) from Cell Signaling Technology was used to detect phosphorylated erbB2 in the SKOV3 model. Total erbB1 was detected using anti-EGFR (sc-03) from Santa Cruz Biotechnology and total erbB2 was detected using anti-Her2/erbB2 from Cell Signaling Technology. Immunoblotting procedures followed those described above. Results were quantitated by densitometry using ImageQuant 5.0 software on a Molecular Dynamics Personal Densitometer SI. Results were expressed as a percentage of the signal compared with the time-matched control after normalizing for total erbB protein in each sample.

Pharmacokinetic Assessments

Male Sprague-Dawley or Wistar rats (Charles River Laboratories), male purebred beagle dogs (Covance), and male cynomolgus monkeys (Biomedical Resources Foundation/Charles River Laboratories) were used for pharmacokinetic assessments. Animals were housed and maintained in accordance with Pfizer Institutional Animal Care and Use Committee, State, and Federal guidelines for the humane treatment and care of laboratory animals. All protocols involving animals were approved by the Pfizer Research and Development Institutional Animal Care and Use Committee. All animals were fasted overnight prior to dosing the next morning, and food was withheld until 4 h following dosing. Water was allowed *ad libitum* throughout the studies. For each study, blood samples were collected from a jugular cannula into EDTA/ascorbic acid tubes. Sampling occurred prior to dosing and at time points up to 144 h after the i.v. and the p.o. dose. To assess the concentration of PF-00299804 or CI-1033 in plasma or human tumor xenograft powders, protein was precipitated with acetonitrile (50 μL of plasma or 50 μg of tumor powder + 150 μL of acetonitrile), and 100 μL of sample was dried down under a steady stream of nitrogen. Samples were reconstituted with 100 μL of mobile phase [40:60 acetonitrile/10 mmol/L ammonium formate (pH 3.5) with formic acid]. Liquid chromatography-tandem mass spectrometry was conducted using a Sciex API 4000 equipped with a Leap Technologies CTCPAL autosampler and a Shimadzu LC-10Avp Pump.

Results

PF-00299804 Irreversibly Inhibits EGFR Kinase Activity

To experimentally confirm the irreversible nature of PF-00299804, 167 nmol/L of purified enzyme was preincubated for 30 minutes with 825 nmol/L of PF-00299804. The enzyme/inhibitor mixture was diluted 167-fold then evaluated in an ELISA-based enzyme assay. Under these

assay conditions, PF-00299804 was diluted to levels below its IC_{50} in the final assay conditions to allow for enzyme activity to return near control levels if the compound bound reversibly. In samples pretreated with PF-00299804, <10% of erbB enzyme activity was recovered following dilution (Fig. 1A), unlike the reversible kinase inhibitor staurosporine in which >70% of the erbB enzyme activity was recovered under identical assay conditions.

PF-00299804 Irreversibly Inhibits Autophosphorylation of EGFR in Cells

PF-00299804 inhibited erbB1 autophosphorylation in the A431 human squamous cell carcinoma line with an IC_{50} of 15.1 nmol/L (Fig. 1B). A second experiment was conducted using the A431 cells to assess the irreversible nature of PF-00299804 inhibition. Cells were exposed to 2 μmol/L of PF-00299804 for varying lengths of time (1–120 min). Medium containing the inhibitor was then removed, and cells were extensively washed for up to 2 hours. When cells were stimulated with EGF, no erbB phosphorylation was detected in cells exposed to PF-00299804 for as little as 1 minute. The reversible EGFR inhibitor erlotinib did not show inhibitory activity under the same assay conditions (Fig. 1C).

PF-00299804 Has Potent Antitumor Activity in Human Tumor Xenograft Models Expressing erbB Family Members

PF-00299804 was evaluated along with CI-1033 in a variety of human tumor xenograft models that express or overexpress erbB family members. PF-00299804 exhibited antitumor effects superior to CI-1033 in three different xenograft models (Table 1). In these models, the therapeutic activity of PF-00299804 ranged from delayed progression to complete regressions. PF-00299804 was most active in models that overexpressed erbB family members, and the inhibitory effects lasted throughout the compound administration. PF-00299804 was tolerated at doses as high as 30 mg/kg in all models evaluated. At this dose, an average of 19% mean body weight loss (from initial body weight at study initiation) was observed (with no lethality). All body weight loss was recovered following cessation of treatment.

In experiments using the SKOV3 human ovarian carcinoma xenograft, which dramatically overexpresses erbB2 along with detectable levels of erbB1, erbB3, and erbB4 (27), PF-00299804 and CI-1033 were given p.o. once per day for 14 days. CI-1033 was marginally active in this model, exhibiting an average tumor growth delay of 6.5 days.

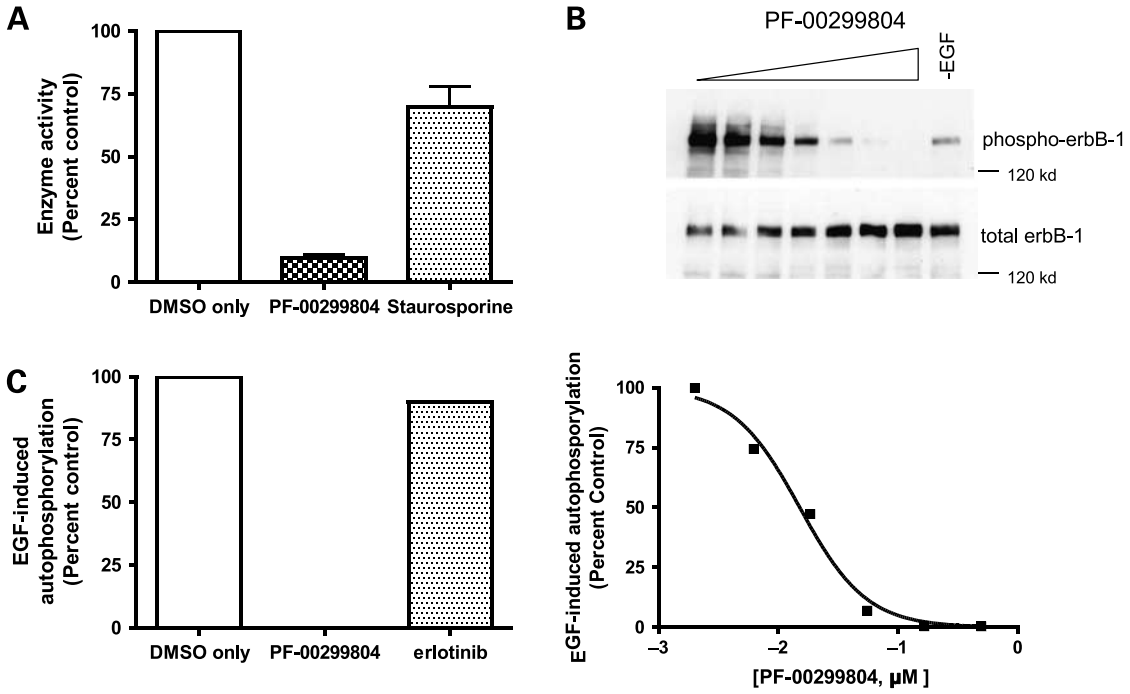

Figure 1. PF-00299804 irreversibly inhibits erbB1 activity *in vitro*. **A,** a GST-erbB1 enzyme/inhibitor mixture was preincubated on ice for 30 min at 167× concentration. The enzyme/inhibitor mixture was then diluted to 1× concentration, and enzyme activity was assessed as described in Materials and Methods. Enzyme activity was not significantly recovered in samples preincubated with PF-00299804. *Columns,* mean; *bars,* 1 SD ($n = 3$). **B,** A431 cells were treated with varying concentrations of PF-00299804 (2, 6.2, 18.5, 55.6, 166.7, and 500 nmol/L) for 2 h followed by EGF stimulation (20 ng/mL) for 5 min. Cells were lysed, proteins were separated by SDS-PAGE, and phosphorylated erbB1 (Tyr^{1068}) was detected using Western blotting techniques. The phosphorylated erbB1 signal was quantitated using densitometry and normalized to total erbB1. Data were graphically displayed as a percentage of activity relative to DMSO controls using GraphPad Prism 4.00, and IC_{50} curves were fitted using a nonlinear regression model with a sigmoidal dose-response. PF-00299804 inhibited EGF-induced autophosphorylation in A431 cells with an IC_{50} = 15.1 nmol/L. Full-length blots are presented in Supplemental Fig. S1. **C,** A431 cells were pretreated with 2 μmol/L of drug for 1 min and then extensively washed for 2 h before stimulation with EGF ligand. PF-00299804 was able to completely inhibit EGF-induced autophosphorylation in A431 cells after 1 min of exposure. *Columns,* percentage of phosphorylation relative to the DMSO controls. Results were reproduced in at least two independent experiments.

However, treatment with PF-00299804 led to tumor growth delays that ranged from 17.1 days (15 mg/kg) to 41.2 days (30 mg/kg). Complete tumor regressions were observed at doses as low as 15 mg/kg of PF-00299804. At the maximum tolerated dose of 30 mg/kg, there were six of six complete tumor regressions seen with PF-00299804 (Table 1; Fig. 2A). Incorporated into this study were experiments evaluating concentrations of PF-00299804 and CI-1033 in tumor samples and the effects of these compounds on erbB2 phosphorylation. Following two daily doses of the efficacious and tolerated dose of 30 mg/kg PF-00299804, tumor concentrations ranged from an average of 5.8 μg/mL (48 hours post-dose) to 40 μg/mL (6 hours post-dose; Table 2). ErbB2 phosphorylation at Tyr^{1248} was inhibited an average of 67%, 99%, and 65% at 6, 24, and 48 h after dosing with 30 mg/kg of PF-00299804, respectively (Fig. 2B). In contrast, tumor concentrations of CI-1033 from mice given 40 mg/kg of CI-1033 once a day for 2 days could only be detected 6 hours after dosing and at significantly lower levels (0.4 μg/mL; Table 2). CI-1033 only inhibited phosphorylated-erbB2 by 56%, 64%, and 62% at 6, 24, and 48 hours post-dose, respectively (Fig. 2B).

In experiments using the A431 human squamous cell carcinoma xenograft model which overexpresses erbB1 and also expresses erbB2 and erbB3 (27), PF-00299804 and CI-1033 were given p.o. once a day for 14 days. Antitumor effects were seen with both compounds but were much more dramatic with PF-00299804 in which an average tumor growth delay of 21 days was observed at doses as low as 1.2 mg/kg. At 11 mg/kg of PF-00299804, one of eight complete regressions and two of eight partial regressions were observed along with a tumor growth delay of >45 days. CI-1033 showed antitumor activity against the A431 human tumor xenograft at a 40 mg/kg dose, in which an average tumor growth delay of 26.6 days was observed along with two of eight partial regressions (Table 1). Inhibitor concentrations in tumors were also assessed in this model. After two daily doses of 33 mg/kg PF-00299804, tumor drug concentrations ranging from 1.1 μg/mL (48 hours post-dose) to 10.8 μg/mL (6 hours post-dose) could be detected. In contrast, CI-1033 given once a day for 2 days at a 40 mg/kg dose could only be detected in tumors 6 hours after dosing and at significantly lower levels (0.2 μg/mL), similar to what was seen with the SKOV3 model (Table 2).

Finally, PF-00299804 and CI-1033 were evaluated in the H125 human NSCLC cell line that expresses erbB2 and erbB3 (in-house observations). After 14 days of p.o. daily dosing, a tumor growth delay of 9.1 days was observed at 30 mg/kg PF-00299804. CI-1033 was not active in this model (Table 1).

Table 1. Spectrum of antitumor activity for PF-00299804 given p.o. in nonclinical human tumor xenograft models

Tumor*	Dose of PF-00299804 (mg/kg)	Schedule	Weight change (%)†	CR‡	PR§	TGD‖
SKOV3¶	65	qDX14	−23.6 (41)	6/6	0/6	79.3**
	30		−19.9 (35)	6/6	0/6	41.2**
	15		−15.8 (35)	2/6	3/6	17.1**
	7.5		−8.0 (28)	0/6	0/6	2.3
	40 mg/kg of CI-1033		−8.1 (35)	0/6	0/6	6.5
	Lactate		−1.9 (28)	0/12	0/12	
A431††	100	qDX14	−20.0 (34)	3/8	2/8	>69**,‡‡
	33		−18.4 (34)	0/8	1/8	50.0**
	11		−5.1 (34)	1/8	2/8	45.1**
	3.7		+	0/8	1/8	30.3**
	40 mg/kg of CI-1033		−4.0 (34)	0/8	2/8	29.6**
	Lactate		+	0/8	0/8	
H125§§	65	qDX14	−19.5 (41)	0/8	0/8	10.2‖‖
	30		−19.4 (37)	0/8	0/8	9.1‖‖
	15		−11.3 (37)	0/8	0/8	3.6
	7.5		−4.9 (27)	0/8	0/8	1.7
	40 mg/kg of CI-1033		−9.0 (37)	0/8	0/8	3.8
	Lactate		−3.4 (27)	0/16	0/16	

*In all experiments, severe combined immunodeficiency mice bore subcutaneous tumor implants. Treatment was initiated when tumors were 200 to 250 mm^3. Animals per group ranged from 6 to 16 mice.

†Percentage of maximum weight change from mean group weight at initiation of treatment. Numbers in parentheses represent the day maximum percentage of weight change was observed.

‡A complete response represents a tumor that decreased in mass at least 75% compared with the tumor mass at initial treatment (e.g., <60 mm^3).

§A partial response represents a tumor that decreased in mass by at least 50% compared with the tumor mass at initial treatment.

‖Tumor growth delay (TGD) is the difference, in days, for the median treated and control tumors to reach a fixed evaluation size (750 or 1,000 mm^3).

¶SKOV3 is a human ovarian carcinoma that overexpresses erbB-2. See Fig. 2A for tumor growth curves.

**Tumor growth delay significantly increased ($P < 0.001$ by one-way ANOVA) relative to the control group.

††A431 is a human squamous cell carcinoma that overexpresses erbB-1. See Supplemental Fig. 3A for tumor growth curves.

‡‡Two out of eight animals were tumor-free 60 d after the last day of dosing.

§§H125 is a NSCLC that expresses erbB-2 and erbB-3. See Supplemental Fig. 3B for tumor growth curves.

‖‖Tumor growth delay significantly increased ($P < 0.05$ by one-way ANOVA) relative to the control group.

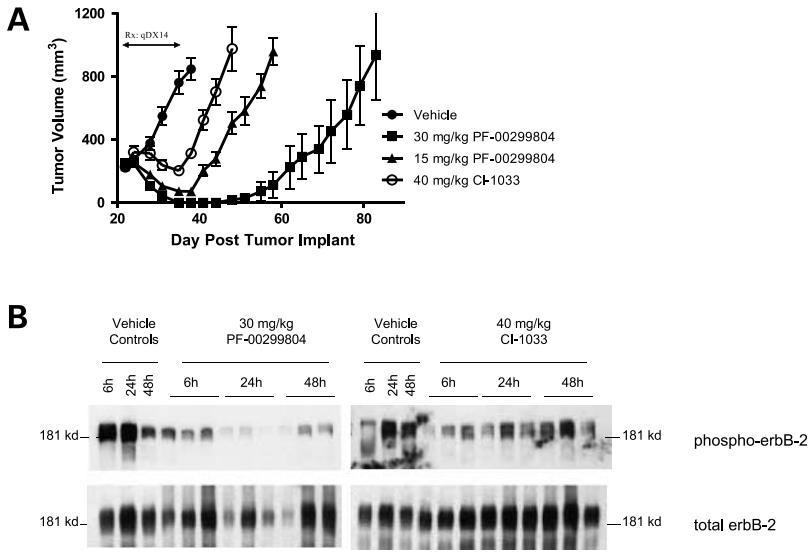

Figure 2. Therapeutic and pharmacodynamic effects of PF-00299804 and CI-1033 on SKOV3 human ovarian carcinoma xenografts. **A,** female severe combined immunodeficiency mice were implanted s.c. with SKOV3 tumor fragments. Daily p.o. treatment (qDX14) with PF-00299804 or CI-1033 began when tumors reached ~200 to 250 mg. *Points,* mean tumor volume; *bars,* SE (6 mice per treatment group; 12 mice in the vehicle-control group). **B,** female severe combined immunodeficiency mice implanted s.c. with SKOV3 tumor fragments received two daily p.o. treatments of PF-00299804 when tumors reached 200 to 250 mg. Tumors were collected 6, 24, and 48 h after the second dose of compound, and then frozen and ground into powder. Tumor powders were lysed, proteins were separated by SDS-PAGE, and phosphorylated and total erbB2 were detected using Western blotting techniques. Phosphorylated erbB2 (Tyr^{1248}) signal was quantitated using densitometry and normalized to total erbB2 signal. More than 99% inhibition of phosphorylated erbB2 was seen 24 h post-dose (30 mg/kg) of PF-00299804, whereas it was only inhibited by 64% 24 h post-dose in mice given 40 mg/kg of CI-1033. Full-length blots are presented in Supplemental Fig. 2.

PF-00299804 Shows Dramatic Effects *In vitro* and *In vivo* against NCI-H1975 Cells Containing the EGFR L858R, T790M Mutation

To test whether PF-00299804 is able to overcome resistance caused by the T790M mutation, PF-00299804 was evaluated along with gefitinib in MTT proliferation assays using NCI-H1975 cells, which harbor both L858R and T790M mutations in erbB1. As shown in Fig. 3A, NCI-H1975 cells were resistant to gefitinib but sensitive to PF-00299804, with an IC_{50} of 0.2 μmol/L.

PF-00299804 was evaluated *in vivo* along with erlotinib to assess the effect of these inhibitors on the growth of NCI-H1975 bronchoalveolar cancer xenografts in nude mice. PF-00299804, given p.o. daily at 7.5 and 15 mg/kg, resulted in an inhibition of tumor growth on the last day of treatment that was equivalent to 41% and 77% ($P < 0.05$), respectively, whereas erlotinib treatment was ineffective at similar doses (Fig. 3B). Biochemical analysis of tumor lysates obtained from mice on the last day of dosing showed dose-dependent and time-dependent inhibition of phosphorylated erbB1 in PF-00299804–treated groups (Fig. 3C). Inhibition of phosphorylated erbB1 at 2 and 26 hours post-dose was 69% and 78%, respectively, in the 7.5 mg/kg dose group and 91% and 97%, respectively, in the 15 mg/kg dose group. Inhibition of phosphorylated erbB1 was not observed with erlotinib treatment (Supplemental Fig. S4).[6]

PF-00299804 Shows Excellent Pharmacokinetic Properties Across Species

Detailed pharmacokinetic studies with PF-00299804 and CI-1033 were completed in rats, monkeys, and dogs. The results are listed in Table 3. In summary, high bioavailability (>50%), long $t_{1/2}$ (>12 hours), and a large volume of distribution (>17 L/kg) were observed with PF-00299804 across all species tested, whereas much lower values were seen for these end points with CI-1033 (Table 3).

Discussion

PF-00299804 is a second-generation quinazoline-based irreversible inhibitor that is structurally related to CI-1033. It potently inhibits erbB1, erbB2, and erbB4 with IC_{50} values of 6.0, 45.7, and 73.7 nmol/L, respectively (28). It shows excellent potency in *in vitro* cells, and a breadth of activity in a range of *in vivo* human xenograft models. PF-00299804 shows prolonged pharmacodynamic effects *in vitro* and *in vivo* when compared with reversible inhibitors and CI-1033, which is likely due to the irreversible nature of the compound as well as the favorable pharmacokinetic properties it displays across all species tested.

PF-00299804 was rationally designed to be an irreversible inhibitor that could covalently interact with a unique unpaired cysteine residue within the ATP binding pocket of the erbB family of receptor tyrosine kinases. As suggested by the proposed binding mode of PD163393, a 6-acrylamido-4-anilinoquinazoline, the key nucleophilic amino acid in the ATP pocket of erbB1 is Cys^{773} (29). The analogous residues in erbB2 and erbB4 are Cys^{784} and Cys^{778}, respectively (30). The irreversible nature of PF-00299804 was confirmed in the present study using two methods; (*a*) after preincubating recombinant erbB1 enzyme with inhibitor for 30 minutes then diluting the enzyme/inhibitor mixture 167-fold, little enzyme activity could be recovered, and (*b*) after A431 cells were exposed to inhibitor for 1 minute and cells were washed multiple times with inhibitor-free medium over the course of 2 hours, no EGF-induced autophosphorylation could be detected. Covalent interaction of PF-00299804 with the erbB kinase domain seems to be selective of the erbB family members because other enzymes that contain analogous cysteine residues in their ATP pocket (e.g., JAK3; ref. 31) were not inhibited by PF-00299804 (28).

[6] Supplementary material for this article is available at Molecular Cancer Therapeutics Online (http://mct.aacrjournals.org/).

Table 2. Tumor concentrations of PF-00299804 or CI-1033 in nonclinical human tumor xenograft models

Tumor	Compound	Tumor concentration of compound (μg eq/g)*		
		6 h	24 h	48 h
SKOV3†	30 mg/kg PF-00299804	40	11.7	5.8
	15 mg/kg PF-00299804	8.6	4.0	1.0
	7.5 mg/kg PF-00299804	3.0	1.3	0.2
	40 mg/kg CI-1033	0.4	BLQ	BLQ
A431‡	33 mg/kg PF-00299804	10.8	4.2	1.1
	11 mg/kg PF-00299804	4.1	0.6	0.1
	3.7 mg/kg PF-00299804	0.4	BLQ	BLQ
	40 mg/kg CI-1033	0.2	BLQ	BLQ

Abbreviation: BLQ, below the limit of quantitation < 0.0244 μg eq/g.
*Animals were dosed once a day for 2 d. Tumor samples were collected 6, 24, and 48 h after the last dose on day 2. Values represent the average data from three mice of extractable drug that is not covalently bound to receptor or nonspecific targets, as described in Materials and Methods.
†SKOV3 is a human ovarian carcinoma that overexpresses erbB-2.
‡A431 is a human squamous cell carcinoma that overexpresses erbB-1.

One potential advantage offered by the irreversible kinase inhibitor PF-00299804 is its ability to potently inhibit all catalytically active erbB family members. A strong body of evidence indicates that the erbB receptors can act synergistically to transform cells in culture (32–34). Clinical investigations have shown that multiple erbB family members can be expressed in a variety of cancers, and patients with cancers overexpressing more than one family

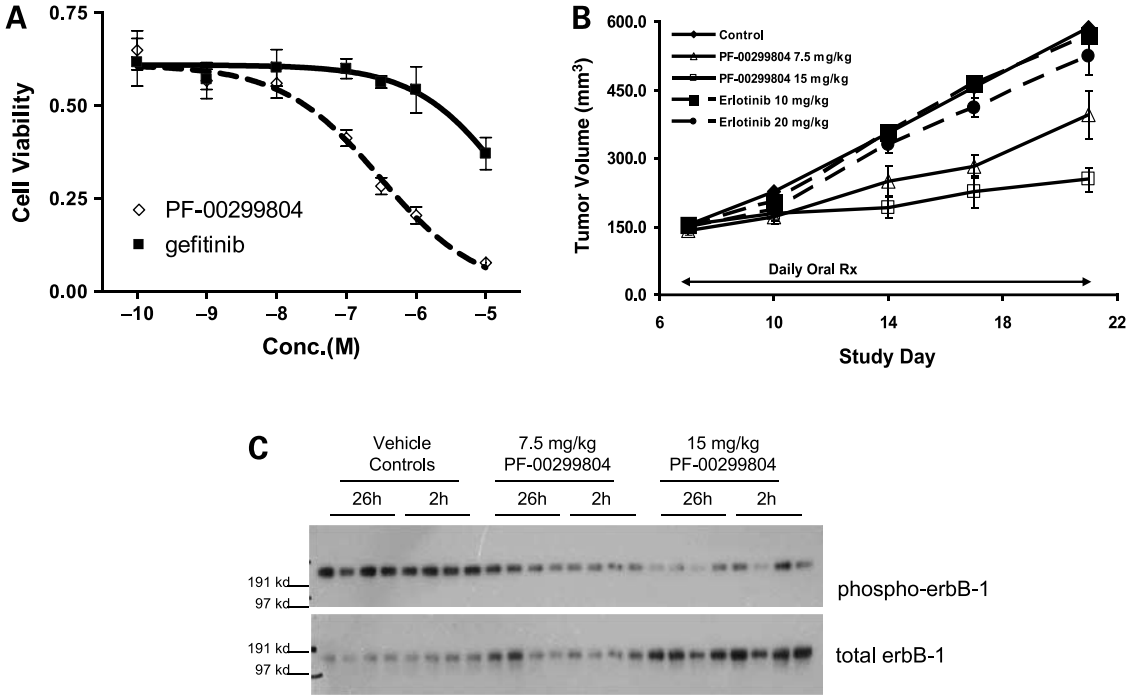

Figure 3. Antiproliferative, therapeutic, and pharmacodynamic effects of PF-00299804 on the NCI-H1975 human NSCLC line harboring the EGFR T790M mutation. **A,** log-phase cells in culture were exposed to varying concentrations of gefitinib or PF-00299804 for 72 h as detailed in Materials and Methods. Cell proliferation was measured using an MTT Cell Proliferation Assay kit obtained from American Type Culture Collection. Data were graphically displayed as a percentage of viability relative to DMSO controls using GraphPad Prism 4.00. IC_{50} curves were fitted using a nonlinear regression model with a sigmoidal dose-response. NCI-H1975 cells were resistant to gefitinib treatment; however, PF-00299084 inhibited the proliferation of NCI-H1975 cells with an IC_{50} of 0.2 μmol/L. **B,** female NCr athymic mice were implanted s.c. with 5×10^6 H1975 cells. PF-00299804 (7.5 and 15 mg/kg) and erlotinib (10 and 20 mg/kg) were given p.o. daily for 14 days, beginning when tumors in mice reached 100 to 200 mg. *Points,* mean; *bars,* SE (eight mice per treatment group). **C,** modulation of phosphorylated EGFR (Tyr^{1068}) by PF-00299804 in NCI-H1975 xenografts was assessed from tumors collected 6 and 24 h after the last dose given in the efficacy study in **B**. Tumor powders were lysed, proteins were separated by SDS-PAGE, and phosphorylated erbB1 (Tyr^{1068}) was detected using Western blotting techniques. Phosphorylated erbB1 signal was quantitated using densitometry and normalized to total erbB1. Total erbB1 was detected using similar Western blotting techniques after stripping the phosphorylated erbB1 blot. Each lane represents an independent excised tumor. More than 95% inhibition of phosphorylated erbB1 was seen 24 h post-dose (15 mg/kg). Full-length blots are presented in Supplemental Fig. 4.

Table 3. Mean pharmacokinetic variables in rat, dog, and monkey

Species	Dose (mg/kg/d)	Route	C_{max} (μg/mL)	AUC* (μg·h/mL)	CL (mL/min/kg)	V_{dss} (L/kg)	$t_{1/2}$ (h)	F (%)
PF-00299804								
Rat†	50	p.o.‡	0.630	20.5			19.4	80
Dog	50§	p.o.‡	0.87	25.2			20.9	74
Monkey	25	p.o.‡	0.217	5.35			12.1	56
Rat†	5	i.v.‖		2.06	49.1	34.2	9.8	
	25	i.v.‖		11.3	32.6	39.8	16.7	
Dog	5	i.v.‖		3.42	24.4	28	15.9	
Monkey	5	i.v.‖		1.90	44.1	17.3	5.7	
CI-1033								
Rat¶	7.86	p.o.‡	0.54	1.19**			1.2	34.6
	39.3	p.o.‡	2.00	6.63			1.4	38.5
Dog	5	p.o.‡	0.098	0.12			0.63	30.5
Monkey	5	p.o.‡	0.013	0.04			2.6	7
Rat¶	1	i.v.‖		0.44	38.2	1.57	0.73	
	5	i.v.‖		1.98	42.1	2.01	1.8	
Dog	5	i.v.‖		0.38	222	10.4	0.81	
Monkey	5	i.v.‖		0.50	167	8.0	1.1	

*AUC (0–144 h) reported.
†Sprague-Dawley rats.
‡p.o. dosing vehicle: 5% PEG200/95% methylcellulose (0.5%) for PF-00299804, 0.5% methylcellulose in water for CI-1033.
§Fed condition, milled to reduce particle sizes.
‖i.v. dosing vehicle: 100% 50 mmol/L of lactic acid (pH 4.0) for PF-00299804, 5% dextrose water adjusted to pH 4.0 with 1.0N HCl for CI-1033.
¶Wistar rats.
**AUC (0–∞) reported.

member have a significantly poorer outcome than those with tumors overexpressing just one family member (35–37). Investigations into the utility of inhibiting both erbB1 and erbB2 *in vitro*, have provided further support for the inhibition of multiple erbB family members (38). Blockade of erbB1 and erbB2 receptors with gefitinib (Iressa) and trastuzumab (Herceptin), respectively, showed synergistic apoptotic effects in the SK-Br-3 and BT-474 breast carcinoma cells, which express multiple erbB family members (39). Synergistic antiproliferative effects were seen with erbB1 and erbB2 blockade using anti-EGFR monoclonal antibody C225 and anti-HER2 monoclonal antibody 4D5 (40). These findings have provided some of the scientific rationale for inhibiting multiple erbB family members either using combination approaches, by designing molecules that have dual erbB1/erbB2 kinase inhibition such as lapatinib, or by designing pan-erbB kinase inhibitors, as can be achieved with the irreversible 4-anilinoquinazolines (29).

In addition to potently inhibiting all catalytically active erbB family members, another attractive property exhibited by PF-00299804 is the prolonged pharmacodynamic effects seen with this compound, *in vitro* and *in vivo*. Suppression of EGF-stimulated erbB1 phosphorylation was achieved in A431 cells for at least 2 hours after only 1 minute of exposure to PF-00299804. Prolonged suppression of erbB1 and erbB2 kinase activity was also seen *in vivo* when PF-00299804 was given to mice implanted with either the H1975 human NSCLC line or the SKOV3 human ovarian carcinoma line. Suppression of erb phosphorylation by ≥97% could be seen for at least 24 hours after dosing with either 15 mg/kg of PF-00299804 in the H1975 line or with 30 mg/kg of PF-00299804 in the SKOV3 line. These pharmacodynamic effects were superior to the effects produced by erlotinib or CI-1033 when these compounds were tested head-to-head with PF-00299804. The excellent pharmacodynamic effects seen with PF-00299804 may be due to the desirable pharmacokinetic properties such as long half-life, high volume of distribution, and high bioavailability that allows for significant distribution of the compound to the tumor and maximal inhibition of erbB activity in cancer cells after once a day p.o. dosing.

Prolonged target suppression, as seen with the irreversible inhibitor PF-00299804, will likely be required for maximum antitumor activity. PF-00299804 showed excellent activity in a variety of xenografts. Partial regressions as well as complete regressions were seen in mice bearing the A431 human squamous cell carcinoma or the SKOV3 human ovarian carcinoma line. Studies have shown that erbB2 expression is rate-limiting for the *in vivo* growth of the SKOV3 tumor, and the turnover of erbB2 in this xenograft line is unregulated (26, 41). It is likely that certain types of human tumors may have fast rates of receptor turnover, as seen with these xenograft lines. Therefore, if significant levels of inhibitor can reach the tumor and remain present, new receptor activity can be inhibited between dosing, and prolonged target suppression can occur, even in tumors that begin synthesizing new receptor within 24 hours.

PF-00299804 is currently in phase I clinical trials (42). Other irreversible erbB inhibitors in development include BIBW-2992 (43) and HKI-272 (44). Both show inhibitory

activity toward erbB1 and erbB2 enzyme. Inhibition toward erbB4 enzyme has not been disclosed for these compounds. The activity of HKI-272 in human tumor xenograft models has also been disclosed (44). This compound shows activity in a variety of human tumor xenografts, including A431, BT474, SKOV3, and those harboring EGFR-activating mutations. In studies with HKI-272, regressions were not seen, which is in contrast to studies with PF-00299804 in which partial or complete regressions were routinely seen in these same models at tolerated doses. *In vivo* pharmacodynamic assessments of HKI-272 evaluating phosphorylated erbB2 in the BT474 model showed complete target suppression lasting only 1 hour after dosing (44), whereas PF-00299804 suppressed phosphorylation of erbB2 by >99% in the SKOV3 human tumor xenograft 24 hours post-dose at a tolerated therapeutic dose in the present study. The superior pharmacodynamic effects and pharmacokinetic properties of PF-00299804 across nonclinical species make this compound an attractive candidate to bring forward into development with the anticipation of superior clinical activity as compared with its competitors and predecessor, CI-1033.

An exciting potential for irreversible inhibitors that has recently come to light is their ability to inhibit mutated forms of EGFR. A variety of mutations in EGFR were identified in patients with NSCLC and included deletions, truncations, and point mutations primarily clustered in the ATP binding pocket of the kinase domain. Many of these mutations have subsequently been shown to lead to the hyperactivity of EGFR tyrosine kinase activity, activation of downstream survival signals, tumorigenesis in cell culture systems, and increased sensitivity to gefitinib and erlotinib *in vitro*, suggesting that these mutations cause the tumor to become dependent on the EGFR signaling pathway for survival (15–17). Unfortunately, most patients with NSCLC containing mutations in the EGFR, which initially respond to gefitinib or erlotinib, ultimately relapse. In patients that have become nonresponsive to these EGFR inhibitors, a common secondary mutation in the EGFR kinase domain, a T790M mutation, has been discovered (20, 21). This mutation is predicted to lead to steric hindrance of gefitinib or erlotinib binding due to a change in the gatekeeper amino acid from threonine to methionine. Methionine has a bulkier side chain that is hypothesized to clash with the substitutions off the aniline head group of gefitinib or erlotinib. Molecular alterations in erbB2 have also been found in NSCLC adenocarcinomas, a glioblastoma, a gastric and an ovarian primary tumor. These somatic mutations include insertions and point mutations in the kinase domain, analogous to those found in EGFR (45–47). Cell lines harboring insertion mutations in the erbB2 kinase domain have been shown to be potent signal transducers, inducing survival, tumorigenicity, and resistance to gefitinib (48, 49). Interestingly, irreversible erbB inhibitors, including PF-00299804, have been reported to work against these mutated receptors (21, 22, 28). Engelman et al. evaluated a variety of cell lines that contain wild-type EGFR and erbB2, or mutations similar to those reported in patients with NSCLC. They have extensively characterized the sensitivity of those lines to gefitinib and PF-00299804 *in vitro*, as well as *in vivo*. Their findings support the use of PF-00299804 in patients with NSCLC that harbor mutations in *EGFR* or *ERBB2*, including those that confer resistance to gefitinib.

We tested PF-00299804 for activity in the H1975 human NSCLC line that harbors the L858R +T790M mutation associated with resistance to reversible anilinoquinazolines (20). When PF-00299804 was compared with gefitinib *in vitro*, PF-00299804 showed the ability to inhibit proliferation of this line at submicromolar concentrations, whereas gefitinib did not. PF-00299804 given p.o. daily also inhibited EGFR phosphorylation and the growth of H1975 xenografts, whereas erlotinib was ineffective at similar doses. These findings support the idea that PF-00299804 may have utility in patients with NSCLC that harbor secondary mutations in their erbB1 receptor, which renders them nonresponsive to erlotinib or gefitinib.

Given the critical importance of erbB receptors in maintaining the neoplastic nature of a variety of cancers and the unmet medical need for the treatment of cancer, clinical evaluation of PF-00299804, an orally available, potent, and highly selective irreversible small molecule inhibitor of the erbB family of tyrosine kinases, may prove to be effective in a variety of human tumors expressing alterations in the erbB receptor family.

Disclosure of Potential Conflicts of Interest

A.J. Gonzales, K.E. Hook, I.W. Althaus, P.J. Harvey, J.M. Nelson, T. Zhu, C.M. Loi, K.M. Schlosser, K.E. Sexton, R.T. Winters, D.J. Lettiere, J. Yang, H.T. Lee and H. Tecle: Pfizer stockholders. The other authors reported no possible conflicts of interest.

References

1. Jorissen RN, Walker F, Pouliot N, Garrett TP, Ward CW, Burgess AW. Epidermal growth factor receptor: mechanisms of activation and signalling. Exp Cell Res 2003;284:31 – 53.

2. Gschwind A, Fischer OM, Ullrich A. The discovery of receptor tyrosine kinases: targets for cancer therapy. Nat Rev Cancer 2004;4:361 – 70.

3. Baselga J, Arteaga CL. Critical update and emerging trends in epidermal growth factor receptor targeting in cancer. J Clin Oncol 2005;23:2445 – 59.

4. Hynes NE, Lane HA. ERBB receptors and cancer: the complexity of targeted inhibitors. Nat Rev Cancer 2005;5:341 – 54.

5. Cohen MH, Williams GA, Sridhara R, Chen G, Pazdur R. FDA drug approval summary: gefitinib (ZD1839) (Iressa) tablets. Oncologist 2003;8: 303 – 6.

6. Cohen MH, Johnson JR, Chen YF, Sridhara R, Pazdur R. FDA drug approval summary: erlotinib (Tarceva) tablets. Oncologist 2005;10: 461 – 6.

7. Moy B, Kirkpatrick P, Kar S, Goss P. Lapatinib. Nat Rev Drug Discov 2007;6:431 – 2.

8. Moyer JD, Barbacci EG, Iwata KK, et al. Induction of apoptosis and cell cycle arrest by CP-358,774, an inhibitor of epidermal growth factor receptor tyrosine kinase. Cancer Res 1997;57:4838 – 48.

9. Wakeling AE, Guy SP, Woodburn JR, et al. ZD1839 (Iressa): an orally active inhibitor of epidermal growth factor signaling with potential for cancer therapy. Cancer Res 2002;62:5749 – 54.

10. Rusnak DW, Lackey K, Affleck K, et al. The effects of the novel, reversible epidermal growth factor receptor/ErbB-2 tyrosine kinase inhibitor, GW2016, on the growth of human normal and tumor-derived cell lines *in vitro* and *in vivo*. Mol Cancer Ther 2001;1:85 – 94.

11. Solit DB, She Y, Lobo J, et al. Pulsatile administration of the epidermal

growth factor receptor inhibitor gefitinib is significantly more effective than continuous dosing for sensitizing tumors to paclitaxel. Clin Cancer Res 2005;11:1983 – 9.

12. Higgins B, Kolinsky K, Smith M, et al. Antitumor activity of erlotinib (OSI-774, Tarceva) alone or in combination in human non-small cell lung cancer tumor xenograft models. Anticancer Drugs 2004;15:503 – 12.

13. Chen J, Smith M, Kolinsky K, et al. Antitumor activity of HER1/EGFR tyrosine kinase inhibitor erlotinib, alone and in combination with CPT-11 (irinotecan) in human colorectal cancer xenograft models. Cancer Chemother Pharmacol 2007;59:651 – 9.

14. Silvestri GA, Rivera MP. Targeted therapy for the treatment of advanced non-small cell lung cancer: a review of the epidermal growth factor receptor antagonists. Chest 2005;128:3975 – 84.

15. Paez JG, Janne PA, Lee JC, et al. EGFR mutations in lung cancer: correlation with clinical response to gefitinib therapy. Science 2004;304: 1497 – 500.

16. Lynch TJ, Bell DW, Sordella R, et al. Activating mutations in the epidermal growth factor receptor underlying responsiveness of non-small-cell lung cancer to gefitinib. N Engl J Med 2004;350:2129 – 39.

17. Pao W, Miller V, Zakowski M, et al. EGF receptor gene mutations are common in lung cancers from ''never smokers'' and are associated with sensitivity of tumors to gefitinib and erlotinib. Proc Natl Acad Sci U S A 2004;101:13306 – 11.

18. Sordella R, Bell DW, Haber DA, Settleman J. Gefitinib-sensitizing EGFR mutations in lung cancer activate anti-apoptotic pathways. Science 2004;305:1163 – 7.

19. Taron M, Ichinose Y, Rosell R, et al. Activating mutations in the tyrosine kinase domain of the epidermal growth factor receptor are associated with improved survival in gefitinib-treated chemorefractory lung adenocarcinomas. Clin Cancer Res 2005;11:5878 – 85.

20. Pao W, Miller VA, Politi KA, et al. Acquired resistance of lung adenocarcinomas to gefitinib or erlotinib is associated with a second mutation in the EGFR kinase domain. PLoS Med 2005;2:e73.

21. Kobayashi S, Boggon TJ, Dayaram T, et al. EGFR mutation and resistance of non-small-cell lung cancer to gefitinib. N Engl J Med 2005; 352:786 – 92.

22. Kwak EL, Sordella R, Bell DW, et al. Irreversible inhibitors of the EGF receptor may circumvent acquired resistance to gefitinib. Proc Natl Acad Sci U S A 2005;102:7665 – 70.

23. Klutchko SR, Zhou H, Winters RT, et al. Tyrosine kinase inhibitors. 19. 6-Alkynamides of 4-anilinoquinazolines and 4-anilinopyrido[3,4-d]pyrimidines as irreversible inhibitors of the erbB family of tyrosine kinase receptors. J Med Chem 2006;49:1475 – 85.

24. Gonzales AJ, Fry DW. G1 cell cycle arrest due to the inhibition of erbB family receptor tyrosine kinases does not require the retinoblastoma protein. Exp Cell Res 2005;303:56 – 67.

25. Corbett TH, Griswold DP, Jr., Roberts BJ, Peckham JC, Schabel FM, Jr. Evaluation of single agents and combinations of chemotherapeutic agents in mouse colon carcinomas. Cancer 1977;40:2660 – 80.

26. Vincent PW, Bridges AJ, Dykes DJ, et al. Anticancer efficacy of the irreversible EGFr tyrosine kinase inhibitor PD 0169414 against human tumor xenografts. Cancer Chemother Pharmacol 2000;45:231 – 8.

27. Moasser MM, Basso A, Averbuch SD, Rosen N. The tyrosine kinase inhibitor ZD1839 (''Iressa'') inhibits HER2-driven signaling and suppresses the growth of HER2-overexpressing tumor cells. Cancer Res 2001;61: 7184 – 8.

28. Engelman JA, Zejnullahu K, Gate CM, et al. PF00299804, an irreversible pan-ERBB inhibitor, is effective in lung cancer models with EGFR and ERBB2 mutations that are resistant to gefitinib. Cancer Res 2007;67:11924 – 32.

29. Fry DW, Bridges AJ, Denny WA, et al. Specific, irreversible inactivation of the epidermal growth factor receptor and erbB2, by a new class of tyrosine kinase inhibitor. Proc Natl Acad Sci U S A 1998;95:12022 – 7.

30. Fry DW. Mechanism of action of erbB tyrosine kinase inhibitors. Exp Cell Res 2003;284:131 – 9.

31. Pan Z, Scheerens H, Li SJ, et al. Discovery of selective irreversible inhibitors for Bruton's tyrosine kinase. ChemMedChem 2007;2:58 – 61.

32. Kokai Y, Myers JN, Wada T, et al. Synergistic interaction of p185c-neu and the EGF receptor leads to transformation of rodent fibroblasts. Cell 1989;58:287 – 92.

33. Dougall WC, Qian X, Greene MI. Interaction of the neu/p185 and EGF receptor tyrosine kinases: implications for cellular transformation and tumor therapy. J Cell Biochem 1993;53:61 – 73.

34. Alimandi M, Romano A, Curia MC, et al. Cooperative signaling of ErbB3 and ErbB2 in neoplastic transformation and human mammary carcinomas. Oncogene 1995;10:1813 – 21.

35. Tateishi M, Ishida T, Kohdono S, Hamatake M, Fukuyama Y, Sugimachi K. Prognostic influence of the co-expression of epidermal growth factor receptor and c-erbB-2 protein in human lung adenocarcinoma. Surg Oncol 1994;3:109 – 13.

36. Xia W, Lau YK, Zhang HZ, et al. Combination of EGFR, HER-2/neu, and HER-3 is a stronger predictor for the outcome of oral squamous cell carcinoma than any individual family members. Clin Cancer Res 1999;5: 4164 – 74.

37. Abd El-Rehim DM, Pinder SE, Paish CE, et al. Expression and co-expression of the members of the epidermal growth factor receptor (EGFR) family in invasive breast carcinoma. Br J Cancer 2004;91: 1532 – 42.

38. Reid A, Vidal L, Shaw H, de Bono J. Dual inhibition of ErbB1 (EGFR/HER1) and ErbB2 (HER2/neu). Eur J Cancer 2007;43:481 – 9.

39. Normanno N, Campiglio M, De LA, et al. Cooperative inhibitory effect of ZD1839 (Iressa) in combination with trastuzumab (Herceptin) on human breast cancer cell growth. Ann Oncol 2002;13:65 – 72.

40. Ye D, Mendelsohn J, Fan Z. Augmentation of a humanized anti-HER2 mAb 4D5 induced growth inhibition by a human-mouse chimeric anti-EGF receptor mAb C225. Oncogene 1999;18:731 – 8.

41. Juhl H, Downing SG, Wellstein A, Czubayko F. HER-2/neu is rate-limiting for ovarian cancer growth. Conditional depletion of HER-2/neu by ribozyme targeting. J Biol Chem 1997;272:29482 – 6.

42. Schellens JH, Britten CD, Camidge DR, et al. First-in-human study of the safety, tolerability, pharmacokinetics (PK), and pharmacodynamics (PD) of PF-00299804, a small molecule irreversible panHER inhibitor in patients with advanced cancer. In: Chicago (IL): American Society of Clinical Oncology; 2007. p. 3599.

43. Agus DB, Terlizzi E, Stopfer P, Amelsberg A, Gordon MS. A phase I dose escalation study of BIBW 2992, an irreversible dual EGFR/HER2 receptor tyrosine kinase inhibitor, in a continuous schedule in patients with advanced solid tumours. In: Atlanta (GA): American Society of Clinical Oncology; 2006. p. 2074.

44. Rabindran SK, Discafani CM, Rosfjord EC, et al. Antitumor activity of HKI-272, an orally active, irreversible inhibitor of the HER-2 tyrosine kinase. Cancer Res 2004;64:3958 – 65.

45. Stephens P, Hunter C, Bignell G, et al. Lung cancer: intragenic ERBB2 kinase mutations in tumours. Nature 2004;431:525 – 6.

46. Shigematsu H, Takahashi T, Nomura M, et al. Somatic mutations of the HER2 kinase domain in lung adenocarcinomas. Cancer Res 2005;65: 1642 – 6.

47. Sasaki H, Shimizu S, Endo K, et al. EGFR and erbB2 mutation status in Japanese lung cancer patients. Int J Cancer 2006;118:180 – 4.

48. Tracy S, Mukohara T, Hansen M, Meyerson M, Johnson BE, Janne PA. Gefitinib induces apoptosis in the EGFRL858R non-small-cell lung cancer cell line H3255. Cancer Res 2004;64:7241 – 4.

49. Wang SE, Narasanna A, Perez-Torres M, et al. HER2 kinase domain mutation results in constitutive phosphorylation and activation of HER2 and EGFR and resistance to EGFR tyrosine kinase inhibitors. Cancer Cell 2006;10:25 – 38.